Asian Journal of Chemistry Vol. 21, No. 2 (2009), 893-902

Computational Study of Transition State of [1,2,5]-Thiadiazolo-[3,4-C]-benzoxadiazole-1-oxide and 3-Oxide with *ab initio* Methods

MAHDI REZAEI SAMETI
Department of Chemistry, Faculty of Science, Malayer University, Malayer, Iran
Fax: (98)(851)3339981; E-mail: mrsameti@gmail.com

ab initio and density functional calculations are used to analyze the transition state optimization and estimating reaction barriers and rate constant of transition state for exchanging oxygen in [1,2,5]-thiadiazolo-[3,4-C]-benzoxadiazole-1-oxide and 3-oxide. All species have been optimized utilizing Gaussian 98 procedure package at the RHF/6-31++G, RHF/6-31++G**, RHF/6-311++G**, B3LYP/6-31++G, B3LYP/6-31G** computational levels. The vibrational mode analysis is used to elucidate the relationships of transition states, intermediates and products. The procedures for finding optimization and verification of transition state structure is quite straightforward and concise. The extensive investigation shows that the reaction mechanism is reliable.

Key Words: Optimization, Transition state, *ab initio*, [1,2,5]-Thiadiazlo-[3,4-c]-benzoxadiazole-1-oxide and 3-oxide, Rate constants.

INTRODUCTION

Potential energy surfaces (PESs) play a central role in computational chemistry. The study of most chemical processes and properties by computational chemists begins with the optimization of one or more structures to find minima on PESs, which correspond to equilibrium geometries. To obtain reaction barriers and to calculate reaction rates using transition state theory (TST)[1,2], it is necessary to locate first-order saddle points on the PES, which correspond to transition states. Often one needs to confirm that a transitions state lies on a pathway that actually connects the minima corresponding to reactants and products (*i.e.* a transitions state that is involved in the chemical process under investigation). This goal is typically accomplished by following the steepest descent reaction pathway downhill in each direction from the TS to the reactant minimum and to the product minimum. The reaction path can also be used in the computation of reaction rates using more sophisticated models such as variational transition state theory and reaction path Hamiltonians (RPH)[3-7]. In some structural properties, atomic arrangements in transition state structures resemble, at the same time, starting materials as well as products or intermediates. Therefore, the transition state is, in fact, a transition from one sate (stationary point) to another. Two structural pairs that are minima on potential energy surface, such as reactants-products. There are many structural transformations (reaction path

ways), that one can envision for the transformation of same reactant into the same products. In almost all cases, chemists are interested in chemical transformation that requires a lower energy demand. These lower energy transformations may have several intermediates that are combined with the same number, plus one more transition state structures. Altogether the reactants, transition state structures, intermediates and products when plotted as energies *versus* bond distances for the bond that is being broken and for the bond is being formed(reaction coordinates), are combined in three dimensional and sometimes many more dimensional potential energy surface.Most computational studies that include potential energy exploration for chemical transformation were performed for molecular systems in the gas phase because molecular solvent is computationally expensive[8-11]. The largest groups of organic reaction that belong to this category is the pericyclic reactions. In these reactions, the bond is simultaneously breaking and forming, or more than one bond is broken and formed at the same time[12]. Therefore reaction transformation are occurring through concerted mechanism. The atomic rearrangement that makes chemical systems such reactants, intermediates, products and transition state structures can be studied computationally. At the present, there are no experimental techniques that can give structural parameters for transition state[13]. Considering the interest in and the importance of transition state structures in understanding almost every chemical transformation, it comes as a surprise that there is no simple computational technique available that explains finding, optimization and verification of transition state structure[14,15].

In this work, based on the RHF and DFT data, the vibrational mode analysis to elucidate the relationships of transition state, intermediates and products *via* the vibrational mode analysis have been used. The extensive investigation shows that the reaction mechanism is reliable. The Gaussian 98 package is used for computing the optimization of reactant, product and transition state for exchanging of oxygen in the [1,2,5]-thiadiazolo-[3,4,c]-benzoxadiazole-1-oxide. This compound is synthesized by method of Boulton *et al.* and is determined that has two conformers[16,17] (Fig. 1).

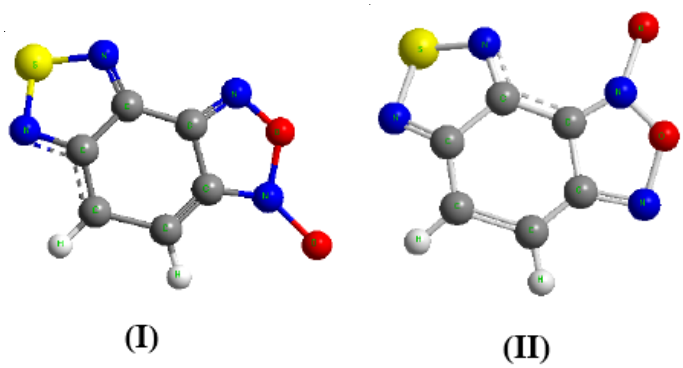

Fig. 1. This figure is a representation of two conformers of (**I**): [1,2,5]-thiadiazolo-[3,4,c]-enzoxadiazole-3-oxide and (**II**): [1,2,5]-thiadiazolo-[3,4,c]-benzoxadiazole-3-oxide

COMPUTATION DETAILS

The optimizations of the reactant, intermediate transition states and products are performed with the Gaussian 98 programs package[18] at the B3LYP/6-311 G** level. The popular hybrid density functional B3LYP method, namely Beck's[19] three-parameter non-local exchange functional with the non-local correlation functional of Lee *et al.*[20], is used throughout the study. Subsequently, connections of the transition states and products are confirmed by intrinsic reaction coordinate (IRC) calculation[21-24]. All the relative energies discussed below are electronic and zero-point energy corrected. The number of imaginary frequencies (0 or 1) confirms a local minimum or a transition state.

RESULTS AND DISCUSSION

The structures of conformer (**I**) and (**II**) are fully optimized at A=RHF/6-31++G, B=RHF/6-31++G** C=RHF/6-311++G**, D=B3LYP/6-31G, E=B3LYP/6-31++G, F=B3LYP/6-31 G**, G= B3LYP/6-31++G** levels of theory. The geometrical parameters for these conformers are depicted in Fig. 1, while the optimized parameters are obtained are listed in Tables 1 and 2. It was observed that the calculated geometry of conformer (**I**), (**II**) have poor agreement with experimental data. This result however is shown in previous work[10]. The deviation between calculated and experimental values are extremely large for bond (C-H): RC-H = 1. 07 A (calc), RC-H = 1. 34 A (experimental) in other bond distances the calculated values are less than observed values.

TABLE-1
OPTIMIZED GEOMETRY (LENGTH OF BOND) FOR TWO CONFORMERS (**I**) AND (**II**); METHODS: A=RHF/6-31++G, B=RHF/6-31++G** C=RHF/6-311++G**, D = B3LYP/6-31G, E=B3LYP/6-31++G, F=B3LYP/6-31 G**, G=B3LYP/6-31++G** K=EXPERIMENTAL [Ref. 9]

	A_I	A_{II}	B_I	B_{II}	C_I	C_{II}	D_I	E_I	F_I	G_I	K_I
R_2(Å)	1.758	1.749	1.629	1.622	1.627	1.620	1.796	1.657	1.793	1.655	1.632
R_3(Å)	1.761	1.762	1.631	1.625	1.629	1.623	1.795	1.655	1.794	1.654	1.633
R_4(Å)	1.278	1.281	1.285	1.289	1.281	1.286	1.318	1.320	1.318	1.321	1.332
R_5(Å)	1.285	1.292	1.291	1.298	1.288	1.295	1.326	1.328	1.326	1.332	1.332
R_6(Å)	1.445	1.462	1.456	1.464	1.456	1.464	1.444	1.446	1.444	1.448	1.460
R_7(Å)	1.460	1.442	1.465	1.443	1.465	1.443	1.451	1.449	1.451	1.449	1.436
R_8(Å)	1.431	1.389	1.421	1.397	1.421	1.395	1.434	1.425	1.435	1.427	1.420
R_9(Å)	1.338	1.343	1.335	1.342	1.333	1.340	1.361	1.359	1.362	1.361	1.362
R_{10}(Å)	1.287	1.297	1.277	1.285	1.274	1.283	1.324	1.314	1.325	1.314	1.314
R_{11}(Å)	1.070	1.069	1.073	1.072	1.071	1.082	1.083	1.082	1.083	1.083	1.211
R_{12}(Å)	1.294	1.380	1.298	1.383	1.298	1.384	1.333	1.336	1.334	1.335	1.320
R_{13}(Å)	1.404	1.221	1.356	1.192	1.350	1.184	1.392	1.365	1.404	1.366	1.420
R_{14}(Å)	1.070	1.071	1.072	1.072	1.073	1.073	1.083	1.083	1.083	1.084	1.340
R_{15}(Å)	1.279	1.179	1.219	1.154	1.210	1.146	1.421	1.218	1.248	1.222	1.417

Table-3 summarizes the thermal parameters such as: the zero-point energy, thermal energy, enthalpy and Gibbs free energy for two conformers (**I**) and (**II**) with

A = RHF/6-31++G , B = RHF/6-31++G** , C = RHF/6-311++G**, D = B3LYP/6-31G, E = B3LYP/6-31++G, F = B3LYP/6-31 G**, G = B3LYP/6-31++G** levels, the result show that the different Gibbs free energy between conformers (**I**) and (**II**) is -88.764 Kcal/mol. The result shows that the conformer of (**I**) is more stable than conformer (**II**) and the exchange from conformer (**II**) to (**I**) is exothermic.

TABLE-2
OPTIMIZED GEOMETRY (ANGLE OF BOND) FOR TWO CONFORMERS (**I**) AND (**II**); METHODS: A=RHF/6-31++G, B=RHF/6-31++G** C=RHF/6-311++G**, D=B3LYP/6-31G, E=B3LYP/6-31++G, F=B3LYP/6-31 G**, G=B3LYP/6-31++G** K=EXPERIMENTAL [Ref. 9,10]

	A_I	A_{II}	B_I	B_{II}	C_I	C_{II}	E_I	F_I	G_I
A_3(°)	92.83	92.813	97.745	97.947	97.647	99.303	99.303	94.458	99.191
A_4(°)	108.26	108.23	107.63	107.78	107.78	107.35	106.05	106.25	106.23
A_5(°)	109.03	109.26	108.46	108.92	108.55	108.99	106.84	106.93	106.99
A_6(°)	127.39	124.26	129.19	125.54	129.32	125.61	127.95	125.80	128.10
A_7(°)	124.25	126.71	125.24	128.03	125.28	128.10	124.62	123.04	124.67
A_8(°)	118.00	117.94	117.07	117.36	117.00	117.34	117.19	118.18	117.31
A_9(°)	120.80	118.36	120.33	117.59	120.35	117.58	120.06	120.56	120.09
A_{10}(°)	130.61	117.42	132.06	117.08	132.23	117.01	130.61	128.63	130.58
A_{11}(°)	117.29	118.80	117.83	119.63	117.81	119.65	118.29	117.89	118.39
A_{12}(°)	106.49	115.03	104.91	114.72	104.75	114.68	106.93	108.81	106.80
A_{13}(°)	105.07	118.42	105.34	117.41	105.56	117.58	106.22	106.65	106.18
A_{14}(°)	122.66	120.77	122.88	120.67	122.87	120.58	122.56	122.02	122.40
A_{15}(°)	132.75	179.00	132.89	178.43	132.94	178.57	135.40	136.45	135.26

TABLE-3
ENERGY OF SPECIES USED IN THIS STUDY IN (hattree/particle) FOR TWO CONFORMERS (**I**) AND (**II**); METHODS: A=RHF/6-31++G , B=RHF/6-31++G** C=RHF/6-311++G**, D=B3LYP/6-31G, E=B3LYP/6-31++G, F=B3LYP/6-31 G**, G=B3LYP/6-31++G**

	Zero point energy	Thermal energy	Enthalpies energy	Gibbs free energy
A_I	-992.739059	-992.730879	-992.729935	-992.773213
A_{II}	-992.676501	-992.667455	-992.666511	-992.711978
B_I	-993.103284	-993.095284	-993.094340	-993.137303
B_{II}	-993.028179	-993.019089	-993.018145	-993.063706
C_I	-993.246689	-993.238632	-993.237688	-993.280760
C_{II}	-993.175081	-993.165953	-993.165009	-993.210639
E_I	-996.997041	-996.987925	-996.986981	-997.031876
F_I	-997.395912	-997.387195	-997.386251	-997.430308
G_I	-997.255822	-997.247033	-997. 246089	-997.290378

After this work we used the Gaussian 98 package with input OPT = (CALCFC, TS) in one step and FREQ keyword in another step for optimization of transition state structure for shifting of oxygen in conformers (**I**) and (**II**). All minima on the potential energy surface have all positive vibrations. The transition state, a saddle point on the potential surface that links two of these stationary points has one imaginary frequency. The imaginary frequency contains atomic movement in the transition

state that in one direction goes to minimum and by movement in the other direction goes to other stationary points that are combined with this transition state structure. Almost all computational methods that are capable of computing transition state structure are based on the simple principle of following the lowest (imaginary) frequency and then finding the maximal point that combines two stationary points. This stationary point should then be optimized and verified. There are many transition state structures but the one that makes the best chemical sense is intermolecular for exchanging of oxygen 1, 2 (Fig. 2). The Harmonic vibrational frequencies of the conformer (**I**) and transition state at the RHF/6-31++G** level is determined in Table-4.

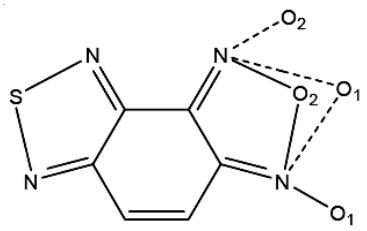

Fig. 2. Transition state structures for oxygen shifting

TABLE-4
OPTIMIZED PARAMETERS OF TRANSITION STATE B (TS) WITH THE CONFORMER B (**I**) AND AT THE RHF/6-31++G** LEVEL; BOND LENGTHS (R) IN (Å), BOND ANGLE (A) AND DIHEDRAL ANGLE (D) IN DEGREE

	R_2 (Å)	R_3 (Å)	R_4 (Å)	R_5 (Å)	R_6 (Å)	R_7 (Å)	R_8 (Å)	R_9 (Å)	R_{10} (Å)	R_{11} (Å)	R_{12} (Å)	R_{13} (Å)	R_{14} (Å)	R_{15} (Å)
B(I)	1.629	1.631	1.285	1.291	1.456	1.465	1.421	1.335	1.277	1.073	1.298	1.072	1.356	1.219
B(TS)	1.632	1.632	1.284	1.289	1.458	1.462	1.461	1.331	1.266	1.073	1.256	1.072	2.346	1.314
	A_3 (º)	A_4 (º)	A_5 (º)	A_6 (º)	A_7 (º)	A_8 (º)	A_9 (º)	A_{10} (º)	A_{11} (º)	A_{12} (º)	A_{13} (º)	A_{14} (º)	A_{15} (º)	
B(I)	97.74	107.63	108.46	129.19	125.24	117.07	120.33	132.06	117.83	104.91	105.34	122.88	132.89	
B(TS)	97.61	107.77	108.14	128.20	125.26	117.15	120.95	128.42	117.96	117.13	117.13	92.02	111.06	
	D_4 (º)	D_5 (º)	D_6 (º)	D_7 (º)	D_8 (º)	D_9 (º)	D_{10} (º)	D_{11} (º)	D_{12} (º)	D_{13} (º)	D_{14} (º)	D_{15} (º)		
B(I)	0.00	0.00	180.00	180.00	180.00	180.00	0.00	0.00	180.00	180.00	180.00	180.00		
B(TS)	0.17	-0.01	179.20	179.92	174.92	178.00	167.22	179.60	-179.8	179.19	147.86	32.76		

The transition state of the abstraction channel is denoted as (Ts) and its geometrical structure is shown in Fig. 2. The comparison of the bond lengths, bond angle and dihedral angle between conformer (I) and transition state at the RHF/6-31++G** level is summarized in Table-5. The incoming O atom attacks one O of conformer(I) from N1 site to N2 site with a slightly bent orientation angle of 111.06 at the RHF/6-31++G** level , the forming N-O bond of 2.346 Å is 73 % longer than equilibrium value of 1.356 Å. Therefore the one bond that should be broken (N1-O2) and bond that should be formed (N2-O1). While all other structural parameters are allowed

to be optimized. The geometry of structural parameters of conformer (**I**) and transition state in summarized in Table-4. The transition state was identified with one negative eigen value of the Hessian matrix and, therefore, one imaginary frequency. Since the imaginary frequency governs the width of the classical potential energy barrier along the MEP, it plays an important role in tunneling calculations, especially when the imaginary frequency is large and the associated eigen vector has a large component of oxygen motion. For the abstraction channel, the imaginary frequency is -655.77 (Table-5), so it is expected that the tunneling effect should be important for the calculation of the rate constant. The comparison of Harmonic vibrational imaginary frequencies, IR intensity and Raman activity of transition state B with the conformer B (**I**) and at the RHF/6-31++G** level is shown in Table-6.

TABLE-5
HARMONIC VIBRATIONAL FREQUENCIES OF THE CONFORMER B (I) AND TRANSITION STATE B (TS) AT THE RHF/6-31++G** LEVEL

Species	Frequency (cm^{-1})
B(I)	101.9308, 157.3464, 244.7772, 268.1576, 296.8740, 68.5917, 437.0002, 479.7943, 529.5441, 535.5776, 626.6839, 636.9576, 699.5149, 709.4298, 754.2834, 814.5550, 820.8196, 837.4680, 870.3030, 894.0165, 914.8386, 960.2698, 1074.9248, 1103.8318, 1151.1351, 1198.4112, 1217.2065, 1332.9680, 1441.3050, 1481.4216, 1505.9100, 1621.1056, 1631.6506, 1715.0705, 1769.6420, 1819.9830, 1864.9756, 3391.9836, 3409.2485
B(TS)	-654.7733, 75.0685, 136.1023, 140.8664, 211.6862, 236.6499, 249.9776, 65.9694, 377.0086, 414.0043, 484.8720, 521.6709, 570.2260, 592.6315, 628.1200, 644.9968, 792.6675, 820.3703, 821.2158, 855.8249, 882.8370, 957.4525, 1091.8344, 1110.5488, 1178.7362, 1298.0400, 1434.2445, 1480.2524, 1514.7904, 1531.8778, 1604.7634, 1731.6121, 1779.6450, 1832.3901, 2293.6132,3392.2778, 3409.0947

TABLE-6
COMPARISON OF HARMONIC VIBRATIONAL IMAGINARY FREQUENCIES, IR INTENSITY AND RAMAN ACTIVITY OF TRANSITION STATE B (TS) WITH THE CONFORMER B (I) AND AT THE RHF/6-31++G** LEVEL

	Frequencies	IR intent	Raman active
B(I)	101.9308	3.0909	0.1703
B(TS)	-978.8048	88.3781	35.5574

In order to further confirm that these transition states connect the designated reactants and products, the intrinsic reaction coordinate (IRC) has been calculated at RHF/6-31++G** level from the transition state to reactants and products. The result of geometry optimized parameter of (IRC) is shown in Table-7.

In the Table-8 the zero point energy, thermal energy, enthalpies energy and Gibbss free energy of conformers (**I**) and (**II**) with transition state structure is compared. According to this data as shown transition state structure is more unstable than

TABLE-7
Z-MATRIX OR GEOMETRICAL PARAMETER OF IRC TEST AT RHF/6-31++G** LEVEL

CD	Cent	Atom	N1	Length/X	N2	α/Y	N3	β/Z	J
1	1	S							
2	2	N	1	1.676303(1)					
3	3	N	1	1.694467(2)	2	95.800(15)			
4	4	C	2	1.308531(3)	1	109.933(16)	3	0.612(28)	0
5	5	C	3	1.306476(4)	1	106.808(17)	2	0.407(29)	0
6	6	C	4	1.527679(5)	2	124.179(18)	1	173.704(30)	0
7	7	C	5	1.471626(6)	3	121.243(19)	1	179.693(31)	0
8	8	C	6	1.588092(7)	4	108.765(20)	2	133.718(32)	0
9	9	C	7	1.399215(8)	6	113.505(21)	4	177.022(33)	0
10	10	H	7	1.130014(9)	5	120.268(22)	3	180.393(34)	0
11	11	H	9	1.086976(10)	8	111.602(23)	5	178.748(35)	0
12	12	N	6	1.282035(11)	4	124.881(24)	2	178.123(36)	0
13	13	N	8	1.453168(12)	6	136.991(25)	4	176.627(37)	0
14	14	O	13	1.686382(13)	8	48.423(26)	6	130.573(38)	0
15	15	O	13	2.750775(14)	8	67.470(27)	6	-58.026(39)	0

TABLE-8
COMPARISON THE ZERO-POINT ENERGY, ENTHALPIES ENERGY, GIBBS FREE ENERGY (hatree/particles) AND ACTIVATION ENERGY (E_a=H(TS)-H(REACTANT) OR E_a=H(TS)-H(PRODUCT); (Kcal/mol)) WITH THE RHF/6-31++G

Compound	ZPE	Enthalpy energy	Gibbs free energy	E_a (Kcal mol^{-1})	ΔH (Kcal mol^{-1})
Reactant(I)	-993.103284	-993.094340	-993.137303	236.405432	
Transition state	-992.676501	-992.666511	-992.711978		88.764267
Product(II)	-992.911363	-992.901888	-992.945803	147.641100	

the compound (**I**). By using the enthalpy of transition state and the conformers [(**I**), (**II**)] the activation energy of forward and backward is calculated and the enthalpy of exchanging conformer (**I**) to conformer (**II**)is determined, the result show in the Fig. 3. The exchange from conformer (**I**) to conformer (**II**) is endothermic.

By using thermodynamic parameters, the rate constant of transition state is calculated. The transition state derived rate constant can be reformulated in thermodynamic terms. Since it is sometimes more useful to work with rate constant in this form than with partition functions. The TST rate constant at a given temperature was calculated using the *ab initio* results as follows:

$$k(T) = l\frac{k_B T}{h}\frac{Q\neq}{Q_R}\exp\left(-\frac{E_o}{RT}\right) \quad (1)$$

where k_B is the Boltzmann constant, Q≠ and Q_R are partition functions for the TS and reactant, respectively, and E_o is the zero-point barrier for reaction. There has been a lot of discussion on reaction path degeneracy[25-27] and the author follows the recommendation by Pollak and Pechukas[26] as summarized by Gilbert and Smith[28]

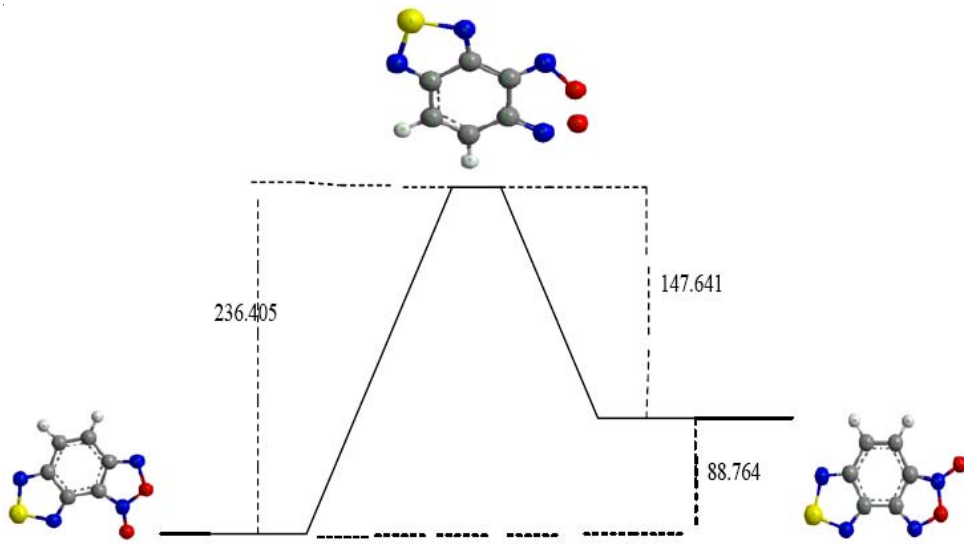

Fig. 3. Structures and relative energies [RHF/6-31++G**//RHF/6-31++G] of the studied reaction sequence in the gas phase

$$l = \frac{m^{\neq}\sigma}{m\sigma^{\neq}} \tag{2}$$

here, σ = symmetry number and m = number of optical isomers and ≠ represents the transition state. If the equilibrium constant is expressed in term of molar Gibbss standard free. The rate expression given by eqn. 3:

TABLE-9
COMPARISON TOTAL CHARGE OF CONFORMER (B(I)) AND TRANSITION STATE (B(TS)) WITH THE RHF/6-31++G

		B(I)	B(TS)
1	S	0.799629	0.784214
2	N	-0.388918	-0.370972
3	N	-0.350731	0.346292
4	C	1.304472	1.311947
5	C	-0.729069	-0.463173
6	C	-1.116585	-0.030497
7	C	0.223744	0.001526
8	C	-0.803424	-1.098640
9	C	0.400014	0.402855
10	N	-0.339028	-0.277100
11	H	0.240221	0.235290
12	N	-0.249534	0.040001
13	O	0.328520	-0.328809
14	H	0.238557	0.244515
15	O	-0.260635	0.169611

$$k = \frac{(k_b T)^2}{h} e^{-\Delta G^{\neq}/RT} \quad (3)$$

in this equation k_h is Boltzman constant, h = Planck constant, the value of rate constants (K) at 298.15 K is equal 2.5572×10^{-8} J/s.

In the Table-9 the comparison total charge of the transition state and compound (**I**) is given, the results show that the sign charge of O_{13} and O_{15} in the compound (**I**) and transition state is reversed and this data is showed that transition state of this processes is rotation of two oxygen synchronize.

Conclusion

Based on great deal of experience with using computational methods for generating and optimizing of stationary state and transition state structure, in present studies a computational procedure by using package Gaussian 98 has been selected. The transition state structure of exchanging of oxygen in the [1,2,5]-thiadiazolo-[3,4-c]-benzoxadiazole-1-oxide to 3-oxide has been determined. It is shown that the transition state structure is more unstable than the compound (**I**). By using the enthalpy of transition state and the conformers [(**I**), (**II**)] the activation energy of forward and backward is calculated and the enthalpy of exchanging conformer (**I**) to conformer (**II**) is determined. The exchange from conformer (**I**) to conformer (**II**) is endothermic. Afterwards, the rate constant for this exchange is also calculated. However, we cannot study the solvent effect on the transition state structure and determined the effect of solvent on the path of reactions.

REFERENCES

1. J.I. Steinfeld, J.S. Francisco and W.L. Hase, Chemical Kinetics and Dynamics, Prentice-Hall, Upper Saddle River, New Jersey (1999).
2. S. Glasstone, K.J. Laidler and H. Eyring, The Theory of Rate Processes; The Kinetics of Chemical Reactions, Viscosity, Diffusion and Electrochemical Phenomena, McGraw-Hill, New York (1941).
3. D.G. Truhlar and B.C. Garrett, *Ann. Rev. Phys. Chem.*, **35**, 159 (1984).
4. D.G. Truhlar, B.C. Garrett and S.J. Klippenstein, *J. Phys. Chem.*, **100**, 12771 (1996).
5. B.C. Garrett and D.G. Truhlar, in eds.: P.V.R. Schleyer, N.L. Allinger, T. Clark, J. Gasteiger, P.A. Kollman, H.F. Schaefer III and P.R. Schreiner, In Encyclopedia of Computational Chemistry, Wiley, Chichester, p. 3094 (1998).
6. W.H. Miller, N.C. Handy and J.E. Adams, *J. Chem. Phys.*, **72**, 99 (1980).
7. E. Kraka, in eds.: P.V.R. Schleyer, N.L. Allinger, T. Clark, J. Gasteiger, P.A. Kollman, H.F. Schaefer III and P.R. Schreiner, In Encyclopedia of Computational Chemistry, Wiley, Chichester, p. 2437 (1998).
8. C. Rangel, M. Navarrete, J.C. Corchado and J. Espinosa-Garcý, *J. Mol. Struct. (Theochem.)*, **679**, 207 (2004).
9. M.Z. Kassaee, M. Koohi and S. Arshadi, *J. Mol. Struct. (Theochem.)*, **724**, 61 (2005).
10. W. Friedrichsen, *J. Mol. Struct. (Theochem.)*, **342**, 23 (1995).
11. A.P. Marchand, Per Cyclic Reactions, Academic Press, New York, Vol. 1 and 2 (1976).
12. J.C. Polanyi and A.H. Zewail, *Acc. Chem. Res.*, **51**, 2657 (1995).

13. B.S. Jursic and Z. Zdravkovski, *J. Mol. Chem.*, **303**, 177 (1994).
14. B. Rajakumar and E. Arunan, *Phys. Chem. Chem. Phys.*, **5**, 3897 (2003).
15. *Chem. Abstr.*, **80**, 140992 (1974).
16. P.B. Ghosh and B.J. Everitt, *J. Med. Chem.*, **17**, 203 (1974).
17. W. Frridrichsen, *J .Mol. Struct.*, **342**, 23 (1995).
18. M.J. Frisch, G.W. Trucks, H.B. Schlegel, P.W.M. Gill, B.G. Johnson, M.A. Robb, J.R. Cheeseman, T.A. Keith, G.A. Petersson, J.A. Montgomery, K. Raghavachari, M.A. Al-Laham, V.G. Zakrzewski, J.V. Ortiz, J.B. Foresman, J. Cioslowski, B.B. Stefanov, A. Nanayakkara, M. Challacombe, C.Y. Peng, P.Y. Ayala, W. Chen, M.W. Wong, J.L. Andres, E.S. Replogle, R. Gomperts, R.L. Martin, D.J. Fox, J.S. Binkley, D.J. Defrees, J. Baker, J.P. Stewart, M. Head-Gordon, C. Gonzales, J.A. Pople, Gaussian 98, Revision A.l,Gaussian, Inc., Pittsburgh, PA (1998).
19. A.D. Becke, *J. Chem. Phys.*, **98**, 5648 (1993).
20. C. Lee, W. Yang and R.G. Parr, *Phys. Rev.*, **B37**, 785 (1988).
21. K. Fukui, S. Kato and H. Fujimoto, *J. Am. Chem. Soc.*, **97**, 1 (1975).
22. K. Ishida, K. Morokuma and A. Komornicki, *J. Chem. Phys.*, **66**, 2153 (1977).
23. Z. Gonzalez and H.B. Schlegel, *J. Phys. Chem.*, **90**, 2154 (1989).
24. H.T. Zhang, Z.Y. Zhou and A.F. Jalbout, *J. Mol. Struct. (Theochem.)*, **663**, 73 (2003).
25. M.R. Wright, Fundamental Chemical Kinetics: An Exploratory, Ellis Horwood, Chichester (1999).
26. E. Pollak and P. Pechukas, *J. Am. Chem. Soc.*, **100**, 2984 (1978).
27. K.J. Laidler, Chemical Kinetics, Harper and Row, New York (1987).
28. R.G. Gilbert and S.C. Smith, Theory of Unimolecular and Recombination Reactions, Blackwell Scientific, Oxford (1990).

(*Received*: 11 August 2007; *Accepted*: 13 September 2008) AJC-6851